Available online at www.sciencedirect.com
SCIENCE DIRECT®
International Journal of Mass Spectrometry 238 (2004) 279–286
International Journal of Mass Spectrometry
www.elsevier.com/locate/ijms

Sequence dependent conformations of glycidyl methacrylate/butyl methacrylate copolymers in the gas phase

Erin Shammel Baker[a], Jennifer Gidden[a], William J. Simonsick[b], Michael C. Grady[b], Michael T. Bowers[a,*]

[a] *Department of Chemistry & Biochemistry, University of California, Santa Barbara, CA 93106-9510, USA*
[b] *DuPont Automotive Finishes, Marshall R&D Laboratory, Philadelphia, PA 19146, USA*

Received 16 September 2003; accepted 15 April 2004
Available online 13 November 2004

Abstract

Sequence dependent conformations of a series of glycidyl methacrylate/butyl methacrylate (GMA/BMA) copolymers cationized by sodium were analyzed in the gas phase using ion mobility methods. GMA and BMA have the same nominal mass but vary in exact mass by 0.036 Da (CH_4 versus O). Matrix assisted laser desorption/ionization (MALDI) was used to form Na^+(GMA/BMA) copolymer ions and their collision cross-sections were measured in helium using ion mobility methods. The copolymer sequences from $Na^+(GMA/BMA)_3$ to $Na^+(GMA/BMA)_5$ (i.e. for the trimer to the pentamer) were studied. Analysis by molecular mechanics/dynamics indicates that each copolymer (regardless of sequence) forms a ring around the sodium ions due to Na^+/oxygen electrostatic interactions. However, the structures vary in size, since the epoxy oxygen atoms in the glycidyl groups are attracted to the sodium ions while the carbon-composed butyl groups are not. This allows copolymers with more GMA segments to fold tighter (more spherically) around the sodium ion and have smaller cross-sections than copolymers with a larger amount of BMA segments in the sequence. Due to this cross-sectional difference, the GMA/BMA sequence compositions of the trimer and tetramer could be quantified.

Keywords: Glycidyl methacrylate/butyl methacrylate; Gas phase; MALDI; Ion mobility

1. Introduction

Synthetic polymers play a very important part in everyday life as well as in industry. They exist throughout the world as materials ranging from nylon fibers in clothing to reinforced plastics. Linking special properties of individual polymers such as viscosity, strength and flexibility is an important part of forming a useful copolymer. As the length of the polymer chain increases more possibilities become available for the polymer. Long polymers form films, are used for sensors, and even allow human existence by creating our genetic code (DNA/RNA). However, it is still important to study the smaller polymers to thoroughly understand the properties of the polymer chains.

Many analytical methods are used to characterize polymer structures. We have developed methods based on mass spectrometry and ion mobility that give detailed information about the conformations of large molecules in the gas phase. Using matrix assisted laser desorption/ionization (MALDI) [1] in conjunction with time-of-flight (TOF) mass spectrometry we are able to characterize which polymers are present in the sample and the abundance of these polymers. By incorporating ion mobility [2,3] into our analysis, we mass-select the ion of interest and analyze it as a function of time as the ion drifts through a cell of buffer gas under the influence of a weak electric field. The amount of time that is takes for the ion to drift is related to its conformation and allows structural analysis of the ion.

* Corresponding author. Tel.: +1 805 893 2893; fax: +1 805 893 8703.
E-mail address: bowers@chem.ucsb.edu (M.T. Bowers).

1387-3806/$ – see front matter © 2004 Elsevier B.V. All rights reserved.
doi:10.1016/j.ijms.2004.04.020

In this paper we report on the application of ion mobility to the structural analysis of glycidyl methacrylate/butyl methacrylate (GMA/BMA) copolymers cationized by sodium with two different end groups, either a hydrogen or vaso end group. In the synthesis of GMA/BMA copolymers, both end groups are produced, however the hydrogen end group is the most abundant. The GMA/BMA copolymers below are named by how many R groups exist in the sequence (i.e. R = 3 is the trimer).

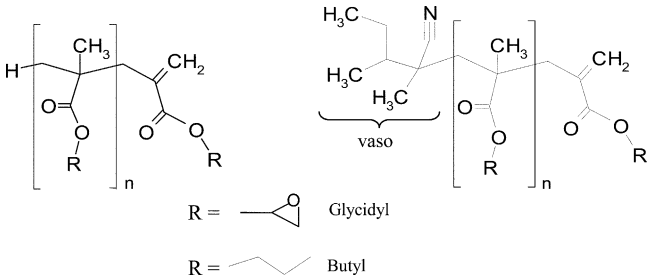

GMA/BMA copolymers incorporate a reactive hydrophilic monomer, GMA, with an inexpensive hydrophobic monomer, BMA. The epoxy group in GMA can be cross-linked to yield long lasting durable films and can also react with nitrobenzoic acid to form dispersants with high affinity for certain pigment surfaces. Similar copolymers with reactive monomers such as GMA have potential applications for high solid content automobile coatings [4]. The problem that results from the attempt to characterize GMA/BMA copolymers is that they have the same nominal mass but a slightly different exact mass (CH_4 versus O) with BMA 0.036 Da larger than GMA. The isobaric distribution due to the different monomer compositions has already been analyzed for these copolymers using FT-ICR [5]. However, this method was only able to indicate the number of GMA or BMA segments but not the position of the segments throughout the copolymer. Ion mobility, on the other hand, analyzes ions depending on size, so different sequences can be quantified as long as a variation in size exists.

2. Experiment

Experiments were performed using a home-built MALDI-TOF instrument. The details concerning the experimental set-up for the mass spectrum and ion mobility measurements have been published previously [6], so only a brief description will be given. Sodiated GMA/BMA copolymers were formed by MALDI in a home-built ion source. 2,5-Dihydroxybenzoic acid (DHB) was used as the matrix and tetrahydrofuran (THF) as the solvent. Approximately 50 μL of DHB (100 mg/mL), 50 μL of the copolymer (1 mg/mL) and 8 μL of NaI (saturated in THF) were applied to the sample target and dried. A nitrogen laser (λ = 337 nm, 12 mW power) was used to generate ions, via MALDI, in a two-section (Wiley-McLaren) ion source. The ions were accelerated down a 1 m flight tube with 9 kV acceleration voltage, while the TOF was operated in reflectron mode to obtain high-resolution mass spectra of the ions formed in the source.

Performing ion mobility experiments requires that the reflectron be turned off and an opposing voltage applied to the ions before the drift cell. By decelerating the ions, collision-induced dissociation is prevented and the ions can be gently injected into the 20 cm long glass drift cell filled with ~1.5 Torr of helium gas. The temperature of the cell can be varied from 80 to 500 K by controlling the flow rate of warmed or cooled nitrogen through passages surrounding the drift cell to meet the needs of the experiment. A weak, uniform electric field across the cell gently pulls the ions through the He gas at a constant drift velocity. After exiting the drift cell, the ions are gently accelerated through a quadrupole mass filter and detected with an electron multiplier. The quadrupole is set to a specific mass-to-charge ratio (m/z) to eliminate any ions that might arise from fragmentation in the drift cell and interfere with the ion mobility experiments. The pulse source extraction voltage triggers a timing sequence so that the ions are detected as a function of time, yielding an arrival time distribution or ATD. The reduced mobility, K_o, of the ion is accurately determined from a series of ATDs measured at different electric field strengths (7.5–16 V/cm) across the drift cell. Through the use of kinetic theory the ion's collision cross-section can also be calculated.

2.1. Data analysis

The reduced mobility of the mass-selected ions can be obtained from the ATD using Eq. (1) [7]:

$$K_o = \left(l^2 \frac{273}{760T} \frac{p}{V} \frac{1}{t_A - t_o} \right) \quad (1)$$

where l is the length of the cell; T, the temperature in Kelvin; p, the pressure of the He gas (in Torr); V, the strength of the electric field; t_A, the ions' arrival time taken from the center of the ATD peak; and t_o is the amount of time the ion spends outside the drift cell before reaching the detector. A series of arrival times (t_A) are measured by changing the voltage (V) applied to the drift cell. A plot of t_A versus p/V yields a straight line with a slope inversely proportional to K_o and an intercept of t_o. Once K_o is found, the ion's collision cross-section can be obtained using Eq. (2):

$$\Omega^{(1,1)} = \frac{3e}{16N_o} \left(\frac{2\pi}{\mu k_b T} \right)^{1/2} \frac{1}{K_o} \quad (2)$$

where e is the charge of the ion; N_o, the number density of He at STP; T, temperature; kb, Boltzmann's constant; and μ is the ion-He reduced mass [7].

2.2. Theoretical modeling

Conformational analysis of the ions is obtained by comparing the experimental cross-section from the ATDs to the cross-sections of theoretical structures. Molecular mechan-

ics/dynamics methods are required to generate the trial structures for large molecules like this copolymer system. We have had success in using the AMBER set of molecular mechanics/dynamics programs [8] to provide reliable structures for many synthetic polymers [9–13]. In these cases, the theoretical cross-sections agreed well with the ion mobility data.

Using the appropriate AMBER parameters, trial structures were calculated for the eight different sequence possibilities for $Na^+(GMA/BMA)_3$, 16 possibilities for $Na^+(GMA/BMA)_4$ and 32 for $Na^+(GMA/BMA)_5$ with both hydrogen and vaso end groups. An annealing/energy minimization cycle was used to generate 100–150 low-energy structures for each copolymer sequence possibility. In this cycle, an initial minimization of the structure is followed by 30 ps of molecular dynamics at 600 K and 10 ps of molecular dynamics in which the temperature is incrementally dropped to 0 K. The resulting structure is then energy minimized again and used as the starting structure for the next minimization/dynamics run. After all 100–150 low-energy structures are obtained, theoretical cross-sections must be calculated for comparison with experimental cross-sections. A temperature-dependent projection model [14,15] with appropriate atomic collision radii calculated from the ion–He interaction potential, is used to calculate the angle-averaged collision cross-section of each theoretical structure. A scatter plot of cross-section versus energy is collected for the minimized structures and used to help identify the ions observed in the experimental ATDs.

3. Results and discussion

A MALDI-TOF mass spectrum of $(GMA/BMA)_n$ doped with NaI is shown in Fig. 1. Only sodiated GMA/BMA ions are observed in the mass spectrum ranging from the trimer to the hexamer for the hydrogen end group and the trimer to the pentamer for the vaso end group. For the ion mobility experiments, all sodiated GMA/BMA copolymer ions are gently injected into the drift cell and their arrival time distributions collected.

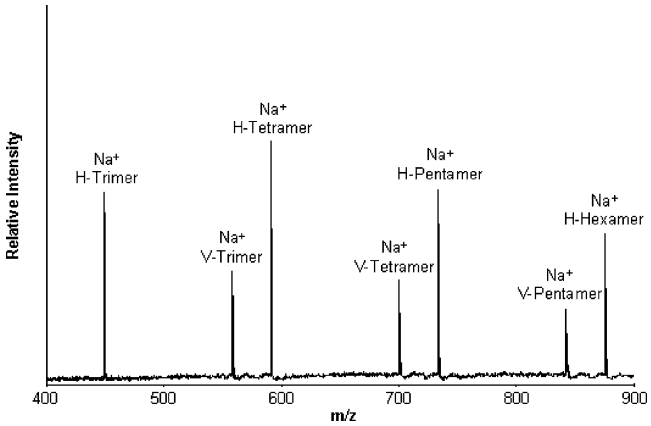

Fig. 1. MALDI mass spectrum of the sodiated GMA/BMA copolymer.

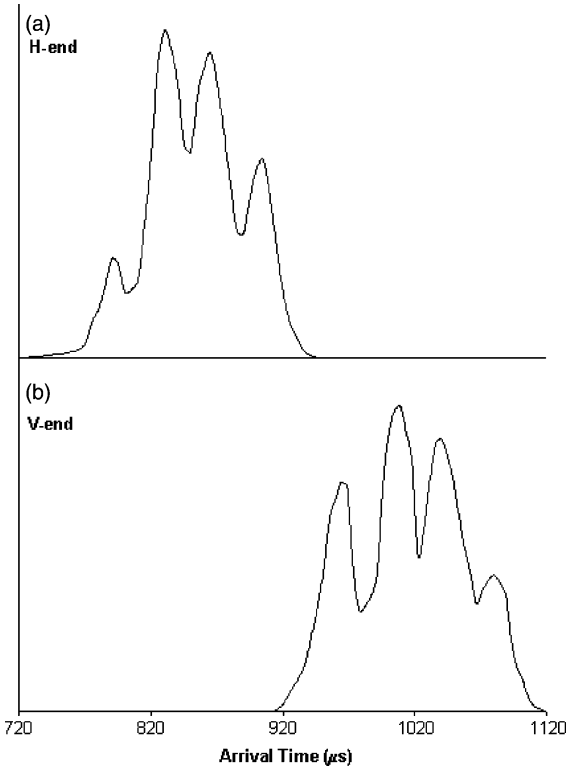

Fig. 2. Arrival time distributions (ATDs) of the trimer for the (a) hydrogen and (b) vaso end groups obtained at a drift cell temperature of 115 K for best resolution. Multiple peaks in the ATDs indicate more than one conformation with different collision cross-sections.

3.1. Na^+ trimer

Fig. 2 shows typical ATDs for the sodiated GMA/BMA trimers. Four resolvable features appear in the ATDs for both the hydrogen and vaso end group. The four peak features indicate four distinct isomers are present, which travel with different mobilities through the helium gas in the ion mobility drift cell. To obtain these ATDs, the temperature of the drift cell was cooled from 300 to 115 K to slow down any possible isomerization and to increase the resolution of the ATD peaks [11,16,17]. This temperature drop did not resolve out any new peaks, indicating isomerization is not likely occurring. The collision cross-sections of each ATD peak were extracted at 300 K using Eqs. (1) and (2) (see ref. [18] for typical t_A versus p/V plots). These values and the relative abundance of each experimental peak are given in Tables 1 and 2 Tables 1 (hydrogen trimer) and 2 (vaso trimer).

Theoretical structures of the sodiated trimer ions were generated using the methods described in the theoretical modeling section. A simulated annealing/energy minimization cycle was used to produce 100 low-energy structures for the trimer (and 150 for the tetra and pentamer) and the angle averaged collision cross-section of each structure was calculated with the projection model. A scatter plot of the cross-section versus energy was then used to help identify the ions observed in the ATDs. A scatter plot obtained for the all GMA

Table 1
Collision cross-sections (Å^2) for hydrogen end trimer

Sequence	Theory (Na^+)	Experiment (Na^+)	% Abundance from ATD
H-GGG	132	130	11
H-GBG	141	139	36
H-BGG	142		
H-GGB	145	146	32
H-BBG	148		
H-BGB	152	153	21
H-GBB	156		
H-BBB	159		0

±1% reproducibility error for experiment; ±2% error for theory.

Table 2
Collision cross-sections (Å^2) for vaso end trimer

Sequence	Theory (Na^+)	Experiment (Na^+)	% Abundance from ATD
V-GGG	161	164	25
V-BGG	163		
V-GBG	171	171	32
V-GGB	176	175	29
V-BBG	178		
V-BGB	181	184	14
V-GBB	186		
V-BBB	191		0

trimer with a hydrogen end group (H-GGG) is illustrated in Fig. 3.

For each sequence of hydrogen- and vaso-end trimers, only one family of low-energy structures is predicted by theory. Representatives for BBB and GGG are shown in Fig. 4. In all cases, the copolymer wraps around the Na^+ ion with all three ester carbonyl oxygens bound to Na^+. However, the overall shape of the copolymer changes depending on the number and sequence of GMA and BMA units. BMA has no additional oxygen atoms, other than the carbonyl oxygens, that can bind to Na^+. Thus, the butyl groups simply extend

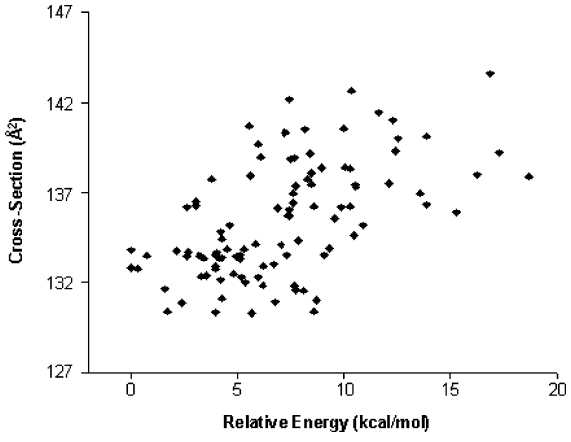

Fig. 3. Scatter plot of cross-section vs. energy for the trimer, H-GGG. Only one family of low-energy structures is predicted for all the GMA/BMA copolymers.

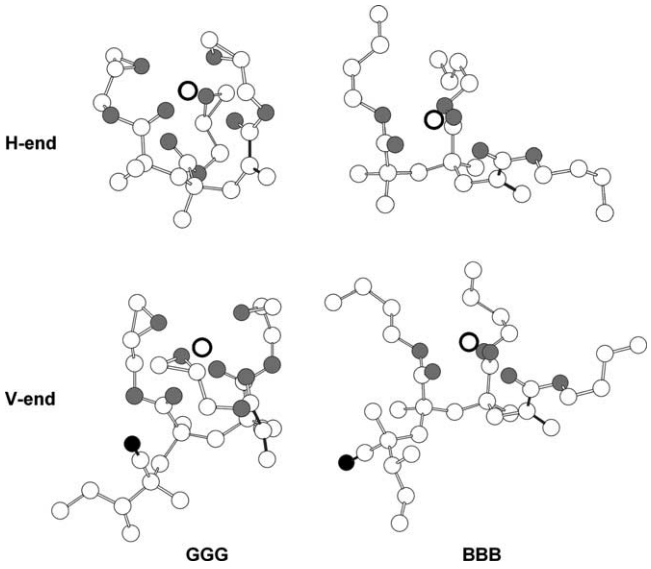

Fig. 4. Lowest energy theoretical structures calculated for the hydrogen and vaso trimers. Only GGG and BBB sequences are illustrated to show the maximum difference in structure. Carbon atoms are white, nitrogen is black, oxygen atoms are grey and sodium is circled (hydrogen atoms have been omitted for clarity).

away from the polymer backbone. GMA, on the other hand, has additional epoxy oxygen that can bind to Na^+. As a result, the glycidyl group folds around the sodium ion. Fig. 4 shows the maximum difference in shape between BMA and GMA by comparing GGG with BBB. For GGG, six oxygen atoms (three carbonyl and three epoxy) coordinate to the sodium ion and the copolymer folds into a ball-like shape. In BBB, only the three carbonyl oxygens coordinate to Na^+ and the polymer forms a more extended structure. As a result, BBB has a 20% larger collision cross-section than GGG (159 ± 3 Å^2 versus 132 ± 3 Å^2 for the hydrogen end group).

For the mixed GMA/BMA trimers, the cross-sections fall between the GGG and BBB values with the trimers containing more GMA segments having smaller cross-sections than those with more BMA segments. The calculated cross-sections for each sequence are listed in Tables 1 and 2. For trimers with one BMA group, sequences with BMA opposite the hydrogen/vaso end have the largest cross-sections. For example, the calculated cross-section of V-BGG is 163 ± 2 Å^2 whereas that of V-GGB is 178 ± 2 Å^2. A similar trend occurs for trimers with one GMA group. The calculated cross-section increases in the order V-BBG < V-BGB < V-GBB (the same trend also holds for the hydrogen end). Since the polymer backbone forms a ring around the sodium ion, placing GMA on the end opposite the hydrogen/vaso end forces the polymer to be more spherical by allowing the sodium ion to coordinate with the epoxy oxygen. However, when BMA is placed on the end opposite the hydrogen/vaso end, the stiffness of the double bond and the extended butyl group force the polymers to be larger and more elliptical in shape as illustrated in Fig. 4.

The calculated collision cross-sections for each trimer sequence possibility are compared to experimental values in Tables 1 and 2. A theoretical cross-section is considered a match to an experimental number if it is within 2% differential [14]. This agreement allows ATD peaks to be assigned. For the hydrogen end trimer, the shortest time peak only matches up with the GGG sequence. The second shortest time peak agrees with a 2 GMA, 1 BMA structure; either BGG, GBG or a combination of the two, but not GGB. The longest time peak corresponds to a 2 BMA, 1 GMA structure; either GBB, BGB or a combination, but not BBG and the experimental cross-section for the second longest time peak agrees with the calculated values of GGB and BBG. The theoretical cross-section of BBB did not fit any of the experimental peaks. The most intense feature in the ATD corresponds to the two GMA, one BMA composition (BGG, GBG or a combination of the two) and so these sequences are probably the most abundant sequences formed in the synthesis of the copolymer. A distinction between the BGG and GBG sequences could not be made on the current instrument due to the small variation in their collision cross-sections.

For the vaso-end trimer, the cross-section from the shortest time peak in the ATD agrees with the calculated values of GGG and/or BGG, while the longest time peak matches BGB and GBB. The second longest time peak most likely contains GGB, BBG or a combination of the two, whereas the second shortest-time peak only corresponds to the GBG sequence. As with the hydrogen-end results, no experimental ATD peaks agreed with the BBB trimer sequence, indicating that BBB was not formed in the synthesis. Also, like the hydrogen-end trimer, the most abundant peak in the ATD corresponds to a two GMA, one BMA copolymer structure (GBG).

3.2. Na^+ tetramer

Typical ATDs for the sodiated GMA/BMA tetramer are shown in Fig. 5. In a similar manner to the trimer studies, ATDs were obtained at 115 K (in addition to 300 K) to improve the resolution. Only the 115 K ATDs are shown in the figure. Four resolvable features appear in the ATD for the hydrogen-end tetramer, but only three features can be resolved for the vaso-end tetramer.

As with the trimer, theory predicts one low-energy family of conformers for each sequence of the tetramer. Representations of the lowest energy structures for GGGG and BBBB are shown in Fig. 6. The sodium ion coordinates to a maximum number of six oxygen atoms. This was also observed for the homopolymer poly (methyl methacrylate) [10] in which the sodium ion bound to a maximum of six oxygen atoms even if more were available for coordination. For BBBB four carbonyl oxygen atoms are available for coordination and all four bind to the sodium ion. GGGG has eight available oxygen atoms (four carbonyl and four epoxy) and tetramer sequences with three GMA, one BMA have seven available oxygens. However, in these situations, the sodium ion binds to only six oxygen atoms on the copolymer. The sodium ion does not discriminate against an epoxy oxygen or a carbonyl oxygen, or among the side closer to the vaso/hydrogen end or the side with the alkene.

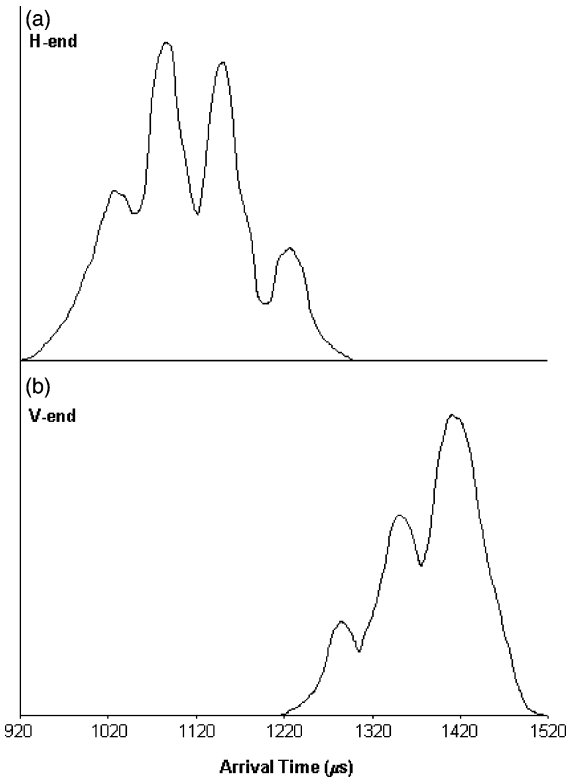

Fig. 5. ATDs of the tetramer for the (a) hydrogen and (b) vaso end groups obtained at a drift cell temperature of 115 K for best resolution.

The calculated cross-sections for each possible sequence of the GMA/BMA tetramer are compared to the experimen-

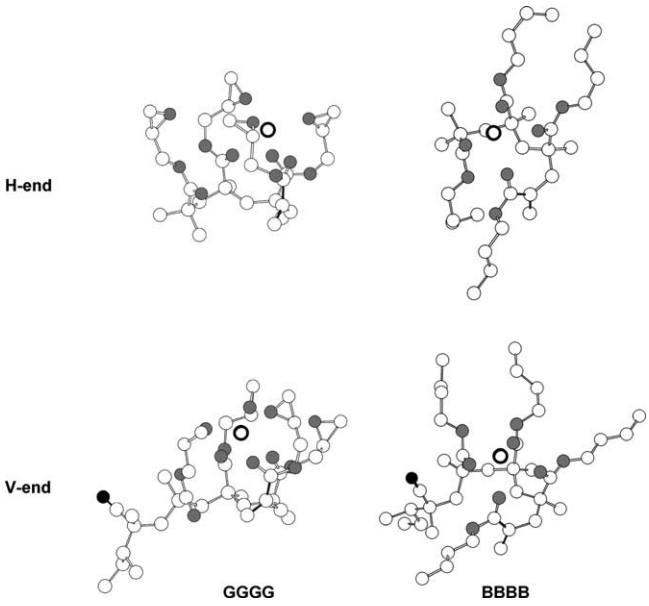

Fig. 6. Lowest energy structures calculated for the tetramer. The GGGG and BBBB sequences are illustrated for the vaso and hydrogen end groups.

Table 3
Collision cross-sections (Å^2) for hydrogen end tetramer

Sequence	Theory (Na^+)	Experiment (Na^+)	% Abundance from ATD
H-GGGG	160	162	19
H-GGBG	166	166	38
H-GBGG	171		
H-BGGG	172		
H-GGGB	173		
H-BBGG	173		
H-BGBG	175		
H-GGBB	175	174	31
H-BGGB	176		
H-GBGB	177		
H-GBBG	177		
H-BGBB	181		
H-BBBG	183	182	13
H-BBGB	184		
H-GBBB	185		
H-BBBB	191		0

tal values in Tables 3 and 4. Similar trends in cross-sectional differences as a function of BMA/GMA composition and sequence were observed for the tetramers as seen for the trimers. In terms of composition, tetramers with more BMA content have larger cross-sections than those with more GMA content. In terms of sequence, the tetramers with only one BMA segment and three GMA segments have the largest cross-section when the BMA group is positioned on the opposite side of the hydrogen/vaso end. When one GMA segment and three BMA segments occur in a tetramer sequence, a similar trend is seen where the sequence with GMA next to the hydrogen/vaso end has the smallest cross-section.

ATD peak assignments for the tetramer are more difficult than the trimer because of the larger number of possible sequences. For the hydrogen end tetramer, the shortest time peak in the ATD (Fig. 5) matches only with GGGG, while the second shortest time peak corresponds to GGBG. The longest time feature matches the four possible sequences of the three BMA, one GMA form: GBBB, BGBB, BBGB, and BBBG. The second longest time peak corresponds to nine possible sequences: six associated with the two GMA, three BMA form and three associated with the three GMA, one BMA form. As seen with the trimers, the theoretical cross-section for BBBB did not fit any of the experimental peaks. These results were synthetically significant because the second shortest time peak, assigned to GGBG, is the most intense peak in the ATD and so it must be a dominant product formed in the synthesis.

Table 4
Collision cross-sections (Å^2) for vaso end tetramer

Sequence	Theory (Na^+)	Experiment (Na^+)	% Abundance from ATD
V-GGGG	186		
V-BGGG	187	188	17
V-GBGG	187		
V-GGBG	194		
V-GGGB	196	197	33
V-BBGG	196		
V-BGBG	196		
V-GBBG	197		
V-GGBB	198		
V-BGGB	204		
V-GBGB	206		
V-BBBG	208	205	50
V-BBGB	208		
V-GBBB	209		
V-BGBB	211		
V-BBBB	218		0

The vaso-end tetramer has a slightly different ATD and peak assignments than the hydrogen-end tetramer. Only three features are resolvable in the ATD and each feature corresponds to more than one sequence. The peak at shortest time agrees with three different sequences, including GGGG, BGGG and GBGG. The peak occurring at intermediate time incorporates the remaining two sequences of the three GMA, one BMA form (GGBG and GGGB) and four possible sequences of the two GMA, two BMA. The peak at longest time is made up of the remaining two sequences of the two GMA, two BMA form (BGGB, GBGB) and three sequences of the three BMA, one GMA form (with the exception of BGBB). In this case, theoretical cross-sections for BGBB and BBBB did not fit any of the experimental peaks.

The most intense peak for the vaso-end tetramer is the peak at longest time, which is made up of a combination of five sequences. For the hydrogen-end tetramer the most abundant sequence is H-GGBG (which is a three GMA, one BMA form), but in the case of the vaso-end tetramer the most abundant sequence(s) consist of two GMA, two BMA and/or one GMA, three BMA forms.

3.3. Na^+ pentamer

One large irresolvable peak appears in the sodiated hydrogen- and vaso-end pentamer ATDs (Fig. 7). Thirty-two sequence possibilities exist, and although the cross-sections of the GGGGG and BBBBB differ by 15%, the other sequences only vary by 1%. Thus, even though multiple isomers (sequences) are undoubtedly present in the pentamer, the high number of possible sequences and their similarity in cross-section outweigh the resolving power of the instrument.

Theoretical structures calculated for the pentamer yield one low energy conformation for each sequence. Representatives of the lowest energy structures for H-GGGGG and H-BBBBB are shown in Fig. 8. The cross-sections associated with these extreme cases are given by the arrows in Fig. 7. One interesting aspect of the pentamer structures is that the maximum number of oxygen atoms the sodium ion binds to is still six (as seen with the tetramer). BBBBB has five oxygen atoms that are able to coordinate to the sodium ion and sequences with only one GMA segment and four BMA segments have six oxygen atoms, so the sodium ion binds to all five or six oxygen atoms. GGGGG, on the other hand, has ten available oxygens (five carbonyl, five epoxy)

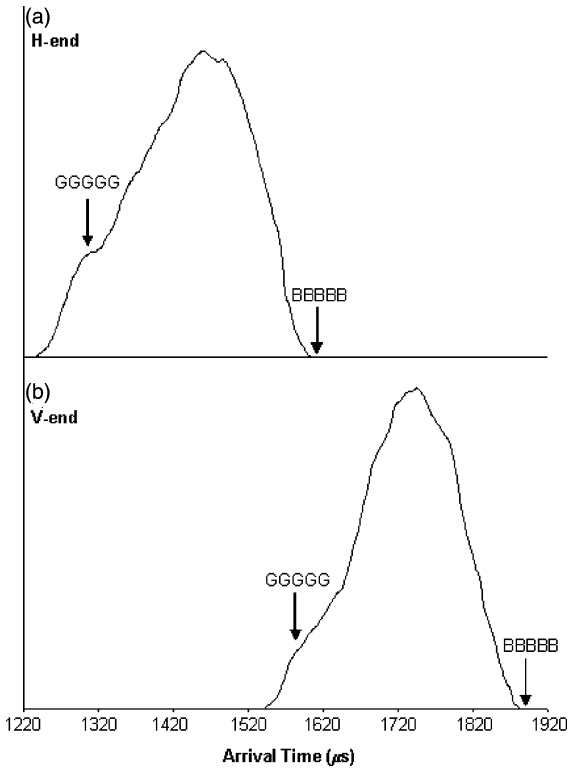

Fig. 7. ATDs for the (a) hydrogen and (b) vaso pentamer obtained at a drift cell temperature of 115 K for best resolution. One irresolvable feature is present due to the small cross-section difference in possible pentamer sequences.

and other pentamers with more than one GMA have more than six oxygen atoms, so the sodium ion must choose were to bind. In PMMA [10], the Na^+ ion bound to two to three carbonyl oxygen atoms on each end of the polymer, forming a U shaped structure. However, in the larger BMA/GMA copolymers, the Na^+ ion binds to only one end of the polymer (either the hydrogen/vaso-end or the alkene end) but not both.

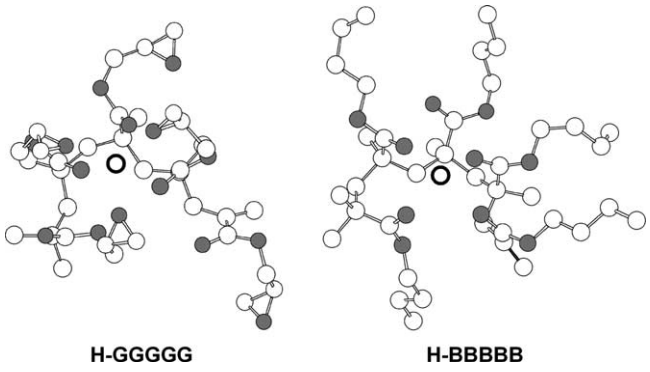

Fig. 8. Lowest energy structures calculated for the hydrogen end pentamer. Only the GGGGG and BBBBB sequences are illustrated to show the difference in sodium binding the GMA and BMA segments.

4. Summary

Mass spectrometry, ion mobility and molecular modeling calculations were used to determine the gas-phase conformations and sequence abundance of sodiated GMA/BMA copolymers ranging from the trimer to the pentamer. Multiple conformations of each copolymer were observed in the ion mobility experiments. Theory predicts one family of conformations for each possible sequence of the copolymers, but the cross-sections of each family differ upon variation in the GMA/BMA composition and sequence. In all cases, the Na^+ ion binds to the multiple carbonyl oxygens in the polymer chain. However, the epoxy oxygens in the GMA units also bind to the Na^+, folding the glycidyl groups around the sodium ion. The butyl groups in the BMA units, on the other hand, do not have any oxygen atoms to bind to the Na^+ and extend away from the polymer backbone. As a result, copolymers with more GMA units yield structures with smaller cross-sections than those with more BMA units. Additionally, copolymers with BMA on the ends cannot fold as tightly as those with GMA on the ends and hence yield structures with larger cross-sections. Based on the theoretical structures, each conformation observed in the ion mobility experiments could be assigned to a particular GMA/BMA composition or sequence. Arrival time distributions for the trimer indicate that the most abundant sequences are the combination of H-BGG and H-GBG for the hydrogen-end group and V-GBG for the vaso-end group. The arrival time distributions for the tetramer indicated that the most abundant sequence is H-GGBG for the hydrogen-end group. There are five sequences for the vaso-end group theoretically corresponding to the most intense peak but these could not be resolved on our instrument. Sequences consisting of only BMA segment (BBB and BBBB) and BGBB in the vaso-end tetramer were the only sequences whose cross-sections did not match any of the experimental values. For all other sequences, theoretical and experimental cross-section agreed within 1–2%. The arrival time distribution for the pentamer yielded one broad irresolvable peak. This result certainly indicates that multiple conformations of the pentamer exist. However, due to the high number of possible sequences for the pentamer and their similarity in cross-section, specific conformations could not be assigned to specific sequences.

Acknowledgement

The support of the Air Force Office of Scientific Research, grant F49620-03-1-0046 is gratefully acknowledged.

References

[1] F. Hillenkamp, M. Karas, R.C. Beavis, B.T. Chait, Anal. Chem. 63 (1991) 1193A.

[2] M.T. Bowers, P.R. Kemper, G. von Helden, P.A.M. van Koppen, Science 260 (1993) 1446.
[3] D.E. Clemmer, M.F. Jarrold, Mass Spectrom. Rev. 32 (1997) 577.
[4] D.D. Weiss, Prog. Polym. Sci. 22 (1997) 203.
[5] S.D.-H. Shi, C.L. Hendrickson, A.G. Marshall, W.J. Simonsick Jr., D.J. Aaserud, Anal. Chem. 70 (1998) 3220.
[6] E.S. Baker, J. Gidden, D.P. Fee, P.R. Kemper, S.E. Anderson, M.T. Bowers, Int. J. Mass Spectrom. 227 (2003) 205.
[7] E.A. Mason, E.W. McDaniel, Transport Properties of Ions in Gases, Wiley, New York, 1988.
[8] D.A. Case, D.A. Pearlman, J.W. Caldwell, T.E. Cheatham III, W.S. Ross, C.L. Simmerling, T.A. Darden, K.M. Merz, R.V. Stanton, A.L. Cheng, J.J. Vincent, M. Crowley, V. Tsui, R.J. Radner, Y. Duan, J. Pitera, I. Massova, G.L. Seibel, U.C. Singh, P.K. Weiner, P.A. Kollman, AMBER 6.0, University of California, San Francisco, 1999.
[9] T. Wyttenbach, G. von Helden, M.T. Bowers, Int. J. Mass Spectrom. Ion Process. 165/166 (1997) 377.
[10] J. Gidden, A.T. Jackson, J.H. Scrivens, M.T. Bowers, Int. J. Mass Spectrom. 188 (1999) 121.
[11] J. Gidden, T. Wyttenbach, J.J. Batka, P. Weis, A.T. Jackson, J.H. Scrivens, M.T. Bowers, J. Am. Soc. Mass Spectrom. 10 (1999) 883.
[12] J. Gidden, T. Wyttenbach, A.T. Jackson, J.H. Scrivens, M.T. Bowers, J. Am. Chem. Soc. 122 (2000) 4692.
[13] J. Gidden, A.T. Jackson, J.H. Scrivens, M.T. Bowers, J. Am. Soc. Mass Spectrom. 13 (2002) 499.
[14] G. von Helden, M.T. Hsu, N. Gotts, M.T. Bowers, J. Phys. Chem. 97 (1993) 8182.
[15] T. Wyttenbach, G. von Helden, J.J. Batka Jr., D. Carlat, M.T. Bowers, J. Am. Soc. Mass Spectrom. 8 (1997) 275.
[16] J. Gidden, M.T. Bowers, Eur. Phys. J. D 20 (2002) 409.
[17] J. Gidden, J.E. Bushnell, M.T. Bowers, J. Am. Chem. Soc. 123 (2001) 5610.
[18] J. Gidden, P.R. Kemper, E. Shammel, D.P. Fee, S. Anderson, M.T. Bowers, Int. J. Mass Spectrom. 222 (2003) 63.